Proc. Natl. Acad. Sci. USA
Vol. 85, pp. 8790–8794, December 1988
Biochemistry

Detection of nucleic acid hybridization by nonradiative fluorescence resonance energy transfer

(oligodeoxynucleotide/base pairing/helix structure/intermolecular distance/intercalators)

RICHARD A. CARDULLO, SUDHIR AGRAWAL, CARLOS FLORES, PAUL C. ZAMECNIK, AND DAVID E. WOLF

Worcester Foundation for Experimental Biology, 222 Maple Avenue, Shrewsbury, MA 01545

Contributed by Paul C. Zamecnik, July 28, 1988

ABSTRACT **Three approaches were used to study hybridization of complementary oligodeoxynucleotides by nonradiative fluorescence resonance energy transfer. (*i*) Fluorescein (donor) and rhodamine (acceptor) were covalently attached to the 5′ ends of complementary oligodeoxynucleotides of various lengths. Upon hybridization of the complementary oligodeoxynucleotides, energy transfer was detected by both a decrease in fluorescein emission intensity and an enhancement in rhodamine emission intensity. In all cases, fluorescein emission intensity was quenched by about 26% in the presence of unlabeled complement. Transfer efficiency at 5°C decreased from 0.50 to 0.22 to 0.04 as the distance between donor and acceptor fluorophores in the hybrid increased from 8 to 12 to 16 nucleotides. Modeling of these hybrids as double helices showed that transfer efficiency decreased as the reciprocal of the sixth power of the donor–acceptor separation R, as predicted by theory with a corresponding R_0 of 49 Å. (*ii*) Fluorescence resonance energy transfer was used to study hybridization of two fluorophore-labeled oligonucleotides to a longer, unlabeled oligodeoxynucleotide. Two 12-mers were prepared that were complementary to two adjacent sequences separated by four bases on a 29-mer. The adjacent 5′ and 3′ ends of the two 12-mers labeled with fluorescein and rhodamine exhibited a transfer efficiency of ≈0.60 at 5°C when they both hybridized to the unlabeled 29-mer. (*iii*) An intercalating dye, acridine orange, was used as the donor fluorophore to a single rhodamine covalently attached to the 5′ end of one oligodeoxynucleotide in a 12-base-pair hybrid. Under these conditions, the transfer efficiency was ≈0.47 at 5°C. These results establish that fluorescence modulation and nonradiative fluorescence resonance energy transfer can detect nucleic acid hybridization in solution. These techniques, with further development, may also prove useful for detecting and quantifying nucleic acid hybridization in living cells.**

In this paper we describe how fluorescently labeled oligodeoxynucleotides (ODNTs) and the process of nonradiative fluorescence resonance energy transfer (FRET) can be used to study nucleic acid hybridization. When two fluorophores whose excitation and emission spectra overlap are in sufficiently close proximity, the excited-state energy of the donor molecule is transferred by a resonance dipole-induced dipole interaction to the neighboring acceptor fluorophore. The results are a decrease in donor lifetime, a quenching of donor fluorescence, an enhancement of acceptor fluorescence intensity, and a depolarization of fluorescence intensity. The efficiency of energy transfer, E_t, falls off rapidly with the distance between donor and acceptor molecule, R, and is expressed as

$$E_t = 1/[1 + (R/R_0)^6], \quad [1]$$

where R_0 is a value that depends upon the overlap integral of the donor emission spectrum and the acceptor excitation spectrum, the index of refraction, the quantum yield of the donor, and the orientation of the donor emission and the acceptor absorbance moments (1, 2). Because of its $1/R^6$ dependence, FRET is extremely dependent on molecular distances and has been dubbed "the spectroscopic ruler" (3).

To follow ODNT hybridization the donor and acceptor fluorophores must be sufficiently close to allow resonance energy transfer to occur. Energy transfer can typically occur up to distances of about 70 Å, or about twice the helix repeat distance in base-paired nucleic acids. We have performed three types of experiments with fluorescently labeled ODNTs. In the first (Fig. 1*a*), two short complementary sequences were labeled with appropriate donor and acceptor molecules at their 5′ ends. In this case resonance energy transfer occurs only between the ends of hybridized ODNTs. The second type of experiment (Fig. 1*b*) involved an unlabeled strand of DNA, which was allowed to hybridize to two shorter, labeled oligonucleotide sequences. Here the "adjacent" 3′ and 5′ ends of the shorter sequences were labeled so that FRET could occur over very short distances upon hybridization. Finally, experiments were performed with the fluorescent dye acridine orange, which intercalates into double-helical nucleic acids and can act as either a donor or acceptor molecule to an appropriate fluorophore covalently attached to a hybridized ODNT (Fig. 1*c*).

We report here that FRET provides a useful means for detection of nucleic acid hybridization in solution. Using this technique, we were able to measure the resonance energy transfer efficiency of ODNT sequences of various lengths as a function of concentration and temperature.

MATERIALS AND METHODS

Chemicals were purchased from Aldrich unless otherwise stated. ODNT synthesis was by the phosphoramidite method using a Biosearch 8600 DNA synthesizer and β-cyanoethyl phosphoramidite (Glen Research, Herndon, VA).

High-performance liquid chromatography (HPLC) was performed with a Waters 600 E gradient programmer and multisolvent delivery system, 481 variable wavelength UV detector, and 745 data module and a Rheodyne 7125 injector. Columns were of the Radial Pak cartridge type of Nova-Pak C_{18} (reversed-phase) or Whatman 10-SAX (ion-exchange) for use with a Z-module system. Elution buffers and programmed gradients used were identical to those reported earlier (4).

Preparation of Fluorescently Labeled ODNTs. *5′-(Aminohexyl)-ODNTs.* An aminohexyl linker was introduced onto the 5′ end of the ODNT by the use of an extra cycle of phosphoramidite synthesis with (9-fluorenyl)methoxycarbonylaminohexyl β-cyanoethyl *N,N*-diisopropylamino phos-

The publication costs of this article were defrayed in part by page charge payment. This article must therefore be hereby marked "*advertisement*" in accordance with 18 U.S.C. §1734 solely to indicate this fact.

Abbreviations: ODNT, oligodeoxynucleotide; FRET, fluorescence resonance energy transfer.

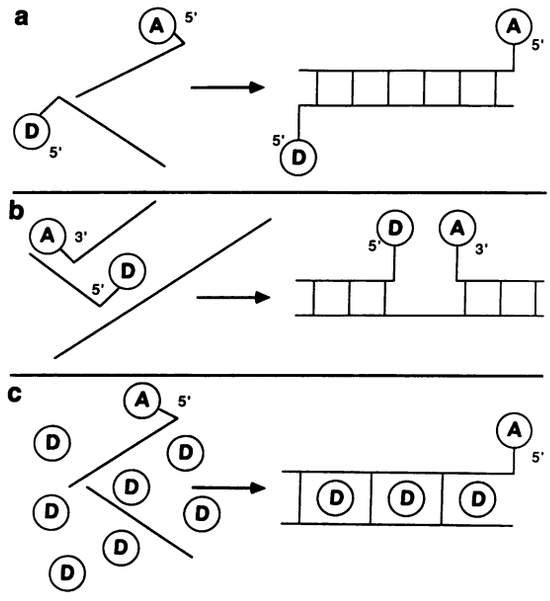

FIG. 1. Strategies for determining nucleic acid hybridization by FRET. (*a*) Fluorescent probes are covalently attached to the 5′ ends of complementary nucleic acids, allowing transfer to occur between a donor (D) and acceptor (A) fluorophore over the length of the hybridized complex. (*b*) Fluorescent molecules are covalently attached to two nucleic acids, one at the 3′ end and the other at the 5′ end. The fluorophore-labeled nucleic acids are complementary to distinct but closely spaced sequences of a longer, unlabeled nucleic acid. (*c*) An intercalating dye is used as a donor for an acceptor fluorophore covalently attached at the 5′ end of one of the nucleic acids.

phite in the coupling reaction (4, 5). After removal of protecting groups with concentrated ammonia solution, the aminohexyl-ODNT was purified by reverse-phase HPLC.

3′-(Aminohexylamino)-ODNTs. The 3′-end derivatization of ODNTs with an amino group is based on established chemistry for 3′-end labeling of RNA (6, 7). To adapt this chemistry for labeling DNA, synthesis of a desired ODNT sequence was carried out on 5′-dimethoxytrityl-3′(2′)-acetylribonucleoside 2′ (3′)-linked to long-chain alkylamino controlled-pore glass support (20 μmol/g; Glen Research, Herndon, VA). After the synthesis, protecting groups were removed in concentrated ammonia. Crude ODNTs were then oxidized with periodate, reacted with 1,6-diaminohexane, and reduced with sodium cyanoborohydride (4, 7). The amino ODNTs were purified by reverse-phase HPLC since they are retarded to a significantly greater extent than underivatized ODNTs.

Attachment of fluorescein and rhodamine to derivatized ODNTs. Attachment of fluorescein, using fluorescein isothiocyanate (Sigma), or tetramethylrhodamine, using tetramethylrhodamine isothiocyanate (Sigma), to the derivatized ODNT and subsequent purification were carried out according to a published procedure (4, 5).

Fluorescence Measurements. Fluorescence measurements were made at the "magic angle" in a Perkin–Elmer spectrofluorimeter (model MPF-3) equipped with a temperature-controlled chamber and Glan–Thompson polarizers. The excitation wavelengths used for fluorescein and acridine orange were 472 nm and 503 nm, respectively. The emission wavelengths used for fluorescein, acridine orange, and rhodamine were 517 nm, 522 nm, and 577 nm, respectively.

In a typical experiment the background fluorescence intensity of 85 μl of phosphate-buffered saline (PBS: 0.138 M NaCl/0.01 M phosphate, pH 7.2) in a 200-μl quartz cuvette (optical solution pathlength = 0.3 cm) was determined. To this cuvette, 15 μl of ≈5 μM donor-labeled or unlabeled ODNT in PBS was added in 5-μl steps and the fluorescence intensity was determined. ODNT containing acceptor fluorophore was then added in 5-μl steps. Energy transfer was observed by both donor quenching and acceptor enhancement. Transfer efficiencies were determined from the quenching data. This involved correcting the data for dilution and for quenching by unlabeled complement. Inner filter effects were negligible. Thus, if $q_{d,u}$ and $q_{d,a}$ are the quenching observed for unlabeled and labeled complements, the transfer efficiency is given by

$$E_t = (q_{d,a} - q_{d,u})/(1 - q_{d,u}). \quad [2]$$

Acceptor-labeled ODNT was added until E_t was constant.

When the intercalating dye acridine orange was used as a donor fluorophore, an unlabeled 12-mer was first added to the cuvette. Acridine orange was then added at a final concentration of 35 μg/ml. The complementary 12-mer, either unlabeled or labeled at its 5′ end, was added last. Data were treated by using Eq. 2.

Most experiments were performed at 5°C. Thermograms to determine the melting temperature, t_m, were made by mixing the ODNTs at 60°C and slowly cooling to 0°C at ≈3°C/min.

RESULTS

Effect of Acceptor Concentration on Transfer Efficiency. To determine the maximum efficiency of transfer between donor and acceptor fluorophores attached to ODNTs, the emission spectrum of acceptor was followed as a function of increasing acceptor concentration at a fixed number of donor molecules. The first experiments were performed using two complementary ODNTs with donor and acceptor fluorophores attached at either end of the hybridized complex: one ODNT had fluorescein attached to its 5′ end (donor), whereas the other, complementary ODNT had rhodamine attached to its 5′ end (acceptor). Quenching and transfer efficiency were determined for ODNTs containing 8 nucleotides, 12 nucleotides, and 16 nucleotides.

Fig. 2*a* shows emission spectra as a function of increasing rhodamine-linked 8-mer concentration to a fixed number of fluorescein-linked 8-mer molecules. As the amount of rhodamine-linked 8-mer was increased, there was a decrease in fluorescein emission intensity (517 nm) and an increase in rhodamine emission intensity (577 nm). Saturation of both the fluorescein quenching and the rhodamine enhancement was complete when the ratio of acceptor to donor exceeded 2:1. The maximum quenching of fluorescein upon saturation was 0.63 in the presence of both donor and acceptor. When the experiment was repeated with fluorescein-linked ODNT and its unlabeled complement, fluorescein emission intensity was quenched 0.26 from its maximum value with no detectable increase in intensity at 577 nm (Fig. 2*b*). Thus, fluorescence was modulated in three ways upon hybridization: a decrease in fluorescein emission upon binding to an unlabeled complementary ODNT, a larger decrease in fluorescein emission intensity upon binding to a rhodamine-linked complementary ODNT, and the detection of rhodamine emission intensity upon binding to a rhodamine-linked complementary ODNT. The first phenomenon represents a quenching of the fluorophore upon binding to its unlabeled complement, while the latter two phenomena represent modulation of fluorescence intensity due to energy transfer. The degree of fluorescein quenching due to energy transfer alone was calculated from Eq. 2. In the case of the 8-mer, the transfer efficiency between fluorescein and rhodamine was therefore about 0.5.

Comparable experiments using 12-mers and 16-mers were also performed (Table 1). In general, the amount of quenching in the absence of acceptor was independent of chain

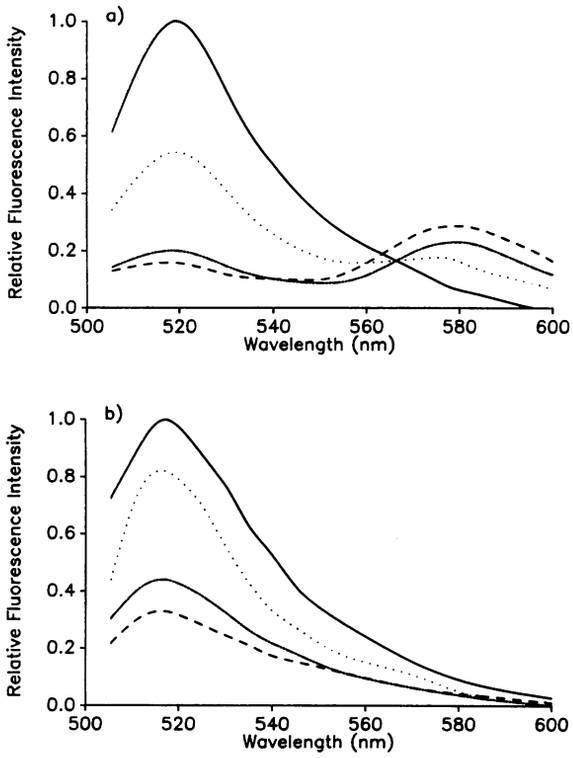

FIG. 2. Modulation of fluorescence intensity upon 8-mer hybridization at fixed numbers of donor molecules and increasing concentration of the complementary ODNT. (*a*) Complementary ODNT was labeled with rhodamine at the 5′ end. Energy transfer occurred between the fluorescein donor and the rhodamine acceptor as shown by a decrease in fluorescein emission intensity at 517 nm and an increase in rhodamine emission intensity at 577 nm with increasing acceptor concentration. (*b*) Complementary ODNT was unlabeled. Curves represent different ratios of rhodamine-linked ODNT to complementary fluorescein-linked ODNT: —, 0:1; ····, 0.40:1; ----, 1.9:1; – – –, 3.8:1. Spectra are not corrected for dilution.

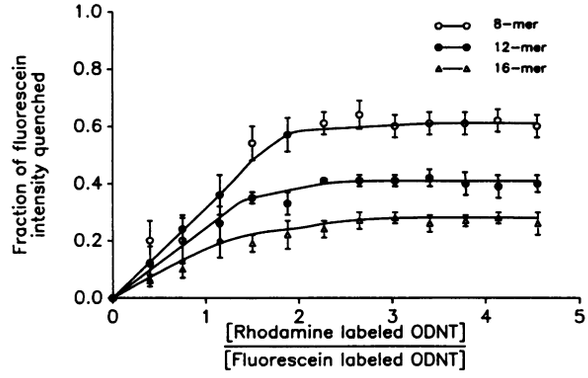

FIG. 3. Transfer efficiency of fluorescein and rhodamine attached to the 5′ ends of complementary ODNTs of various lengths. Transfer efficiency was calculated from the difference in fluorescein quenching in the presence or absence of rhodamine attached to complementary ODNT. The transfer efficiency, E_t, at saturation decreased progressively with chain length from the 8-mer (0.37) to the 12-mer (0.16) to the 16-mer (0.03), reflecting a decrease in efficiency with increasing distance. In each case, saturation occurred at an acceptor/donor ratio of <2:1. The data points are means ± SD for four different experiments.

length and had a value of 0.26 ± 0.02 for all ODNTs (mean ± SD for four determinations of each *n*-mer, where $n = 8$, 12, or 16 nucleotides). In the presence of rhodamine-linked complementary ODNT, the degree of fluorescein quenching due to energy transfer alone decreased with increasing chain length. As shown in Fig. 3, hybridization was complete for all three chain lengths at an acceptor/donor ratio of 2:1. At higher acceptor/donor ratios, no modulation in the corrected fluorescein or rhodamine signal was observed. Subsequent experiments using these ODNTs were done at an acceptor/donor ratio of 4:1 to ensure that hybridization was complete.

Effect of Temperature on Transfer Efficiency. The effect of temperature on hybridization was also followed for different chain lengths (8-, 12-, and 16-mers) at saturating concentrations of acceptor-linked ODNT. The resulting melting temperatures (t_m), defined as the midpoint values of fluorescein quenching or rhodamine enhancement over a temperature range of 0–60°C, were compared with absorbance data at 260 nm. Above 50°C, there was no fluorescein quenching or detectable rhodamine signal (data not shown). As the temperature was lowered the fluorescein intensity decreased and the rhodamine intensity increased in a sigmoidal manner (Fig. 4). This agreed well with the absorbance data, which showed a characteristic sigmoidal decrease in A_{260} with decreasing temperature (Fig. 4).

In general, there was no significant difference between t_m values obtained by fluorescein quenching and by decreased A_{260} signal with decreasing temperature. The t_m values obtained by fluorescein quenching were 23.8 ± 4.2°C, 38.3 ± 4.5°C, and 47.2 ± 5.2°C for the 8-mer, 12-mer, and 16-mer, respectively (mean ± SD for four determinations). By comparison, the t_m values obtained by a decrease in A_{260} were 24.5°C, 37.5°C, and 46.0°C (for the 8-mer, 12-mer, and 16-mer, respectively). Hence, in all cases, the t_m determined by fluorescence was within 3% of the t_m determined by A_{260}.

Hybridization of Two Labeled ODNTs to a Complementary Strand. Experiments were also performed with two fluorescently labeled ODNTs hybridized to a longer complementary strand (Fig. 1*b*). When these three strands hybridize, only four bases separate the fluorescein donor from the rhodamine acceptor. As in the previous experiment, quenching of donor fluorescence by energy transfer increased to saturation with acceptor concentration (data not shown). Table 2, line A, shows the results of these experiments. In the presence of fluorescein-labeled ODNT and unlabeled ODNT hybridized to the 29-mer, the quenching of fluorescein emission was about 0.27. In the presence of rhodamine acceptor, the quenching was enhanced to 0.71 and there was a large fluorescence signal at the rhodamine peak (577 nm). Hence, the transfer efficiency, given by Eq. **2**, was about 0.6.

Energy Transfer with Acridine Orange. The intercalating dye acridine orange was used as a donor to detect hybridization between an unlabeled ODNT and its rhodamine-labeled complement. Fluorescence of acridine orange under-

Table 1. Modulation of fluorescein intensity at saturating levels of ODNT with and without rhodamine attached for ODNTs of chain length *n*

n	$q_{f,r}$	$q_{f,u}$	E_t	R/R_0
8	0.632 ± 0.046	0.265 ± 0.021	0.501 ± 0.035	0.99 ± 0.02
12	0.423 ± 0.030	0.265 ± 0.013	0.215 ± 0.052	1.24 ± 0.05
16	0.295 ± 0.017	0.262 ± 0.013	0.045 ± 0.018	1.66 ± 0.10

Data represent mean ± SD for four different experiments. See Eqs. **1** and **2**. Subscripts f, r, and u indicate fluorescein-labeled, rhodamine-labeled, and unlabeled ODNT.

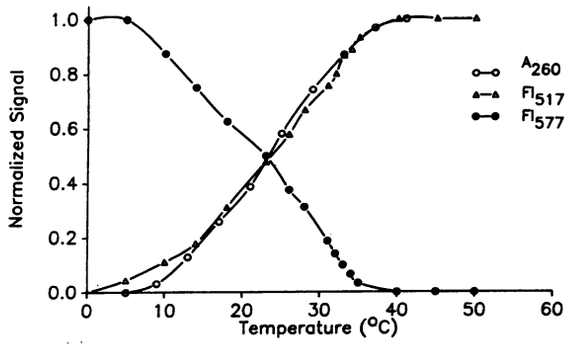

FIG. 4. Changes in fluorescence intensity of donor- and acceptor-linked 8-mers as a function of temperature. When the temperature was decreased from 60°C to 0°C, the fluorescein emission intensity (●) monotonically decreased, indicating an increase in transfer efficiency with the rhodamine acceptor on the complementary 8-mer. In addition to the decrease in fluorescein emission intensity with increasing temperature, there was a concurrent increase in rhodamine emission intensity (△). A_{260} (○) showed a characteristic decrease with decreasing temperature, indicating hybridization of complementary ODNTs.

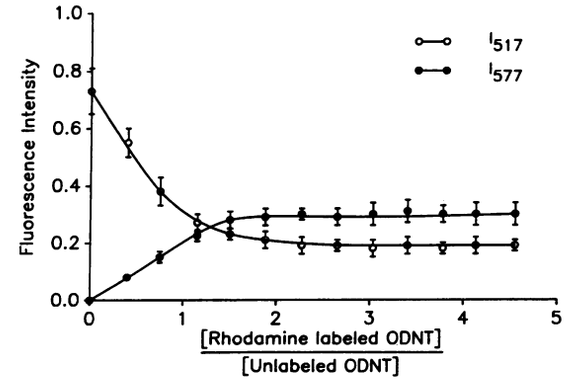

FIG. 5. Changes in fluorescence intensity at 517 nm (○) and at 577 nm (●) as a function of rhodamine-linked ODNT concentration at fixed concentrations of unlabeled complementary ODNT and acridine orange.

goes a spectral shift upon binding of the dye to double-stranded DNA, and this modulation can be used to determine the ratio of single-stranded to double-stranded species in solution (8). In our hybridization studies, when acridine orange intercalated into complementary 12-mers it exhibited an excitation maximum at 503 ± 3 nm and an emission maximum at 522 ± 2 nm.

In these studies, two ODNTs were used: one was unlabeled and its complement was labeled with rhodamine at the 5′ end. Acridine orange was added to the cuvette along with the unlabeled strand at a fixed concentration, and the rhodamine-labeled ODNT was added in various amounts. The degree of fluorescence quenching along with the enhancement of rhodamine fluorescence at 577 nm increased and then leveled off with increasing acceptor concentration (Fig. 5). As expected, unlike the case where single donor and acceptor molecules were covalently linked to ODNTs, the degree of energy transfer was much higher when the intercalating dye was used. Under saturating conditions of acceptor concentration, the quenching of acridine orange approached 0.57 (Table 2, line B). The amount of quenching observed with two unlabeled 12-mers was only about 0.11, so that the resulting transfer efficiency was 0.52. This can be compared to the case of the 12-mers with fluorescein and rhodamine at their respective 5′ ends, which gave a transfer efficiency of only 0.22 (Table 1). Hence, the presence of an intercalating dye along the entire length of the ODNT enhanced the transfer efficiency by a factor of ≈2 in the 12-mer.

DISCUSSION

For detecting nucleic acid hybridization, an ideal fluorescent ODNT probe would (*i*) be easily attached to an ODNT, (*ii*) be detectable at low concentrations, (*iii*) produce a modulated signal when the labeled ODNT hybridized to a complementary ODNT, and (*iv*) be stable at temperatures used in hybridizations (9, 10). In this report we have shown that nonradiative FRET provides a sensitive method for detection of binding between complementary ODNTs.

FRET has been used to quantify the distance between donor and acceptor fluorophores and accurately predicts the distance between donor and acceptor in polymers of various lengths (3). Our studies using complementary ODNTs covalently tagged with fluorescent probes indicate that this technique can be used to investigate certain physical parameters of nucleic acid hybridization. In particular, the distance between the donor and the acceptor, R, can be calculated if it is assumed that the hybridized ODNTs form a helix and if the orientation of the donor and acceptor fluorophores relative to the helical axis is known. From the transfer efficiencies in Table 1, we have calculated the distance between the fluorescein donor and the rhodamine acceptor molecules as a function of base position by using Eq. 1.

As regards the geometry of the fluorophores relative to the helical axis, we have considered three simple models (Fig. 6). In general, the distance between donor and acceptor can be expressed as

$$R = \{2(r + d\cos\varphi)^2\{1 + \cos[(\Delta N + 1)\pi/5]\} + (3.4\Delta N + 2d\sin\varphi)^2\}^{1/2}, \quad [3]$$

where r is the radius of the double helix (10 Å), ΔN is the base separation (0, 1, 2, . . .), d is the length of the probe representing the six-carbon spacer and a phosphate group (≈12.8 Å), and φ is the angle of the spacer from the helical axis ($-\pi/2 \leq \varphi \leq \pi/2$). Model 1 (Fig. 6) assumes that the probes are perpendicular to the helical axis ($\varphi = 0$). In model 2 the probes are parallel to the helical axis and pointing away from the bases at the 5′ end ($\varphi = \pi/2$), and in model 3 the probes are parallel to the helical axis but lie along the helix so that the probes are at closest approach ($\varphi = -\pi/2$). A plot of these calculated R values (from Eq. 3) as a function of $[(1/E_t) - 1]^{1/6}$ should give a straight line with the slope corresponding to R_0 for the donor and acceptor pair as predicted by Eq. 1.

Linear regression of each of the three calculated R values gave a good fit (coefficient of determination $r^2 > 0.9$) only for

Table 2. Quenching and transfer efficiency of two 12-mers attached to a 29-mer (line A) and of two hybridized 12-mers in the presence of acridine orange (line B)

	$q_{d,r}$	$q_{d,u}$	E_t	R/R_0
A	0.712 ± 0.024	0.276 ± 0.012	0.602 ± 0.017	0.933 ± 0.011
B	0.573 ± 0.027	0.109 ± 0.009	0.520 ± 0.016	—

Data represent the mean ± SD for four different experiments. Subscript d represents fluorescein in line A and acridine orange in line B.

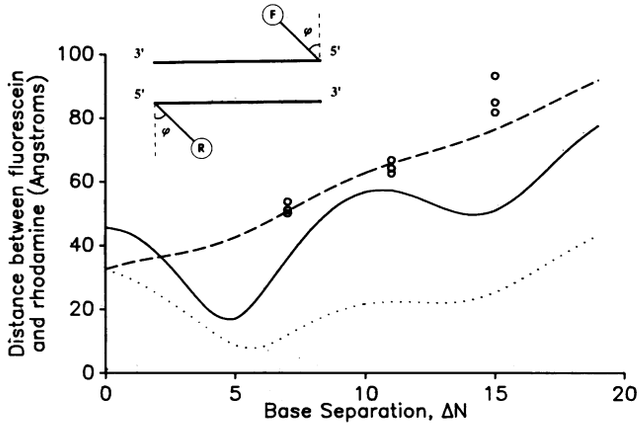

FIG. 6. Distance between donor and acceptor molecules as a function of base separation for different-length ODNTs. Three models of different spacer orientation were tested (*Inset*). The three curves represent the calculated distance between the fluorescein (F) donor and the rhodamine (R) acceptor as a function of base position for each of the three models: —, model 1 ($\varphi = 0$); – – –, model 2 ($\varphi = \pi/2$); ···, model 3 ($\varphi = -\pi/2$). Linear regression of the calculated R values for the 8-mer, 12-mer, and 16-mer as a function of $[(1/E_t) - 1]^{1/6}$ gave a best fit for model 2 (coefficient of determination $r^2 = 0.94$) with a corresponding R_0 of 49.1 Å. By comparison, correction of the published R_0 value for fluorescein and rhodamine attached to long-chain hydrocarbons of 54.2 Å (11) by our observed quenching factor of 0.26 resulted in a value of 52.2 Å. The data points (○) represent the distance between the donor and acceptor molecules obtained by using the corrected R_0 value of 52.2 Å. Again, these data gave a reasonable fit to model 2, suggesting that upon ODNT hybridization, the probes are pointing away from the 5′ ends of the helix.

model 2 (Fig. 6) with a corresponding R_0 of 49.1 Å. By comparison, the published value for fluorescein donors and rhodamine acceptors attached to long-chain hydrocarbons in solution is 54.2 Å (11). However, when one accounts for the quenching that we observed in the absence of acceptor-linked ODNT, a corrected R_0 value of 52.2 Å $[54.2/(1.26)^{1/6}]$ is obtained. Use of this corrected value for R_0 along with our energy-transfer data for the 8-mer, 12-mer, and 16-mer gave a reasonable fit to the values calculated for model 2 (open circles in Fig. 6). Hence, the data support a model in which the probes are pointing away from the 5′ ends of the helix.

In constructing fluorophore end-labeled nucleic acids, it is possible to choose different spacers that will give a range of transfer efficiency values upon hybridization. Multiple determinations of distances with different-length spacers might allow the secondary structure of nucleic acids to be ascertained in solution.

We have also shown that the technique of FRET allows hybridization to be monitored by covalently attaching fluorophores to the 3′ and 5′ ends of ODNTs that can be hybridized to a longer ODNT. In this case, the donor and acceptor molecules can theoretically be separated by only a few base pairs so that energy transfer occurs with very high efficiency upon hybridization. Intercalating dyes provide another method for detecting nucleic acid hybridization by FRET. The use of an intercalating dye allows a short separation distance between donor and acceptor molecules and, in the case of a helical structure, presents many dye molecules at different distances and orientations. The result is an "antenna effect" that gives a high degree of transfer efficiency. Some intercalating dyes, such as acridine orange and ethidium bromide, have the added benefit of changing their spectral properties upon binding to double-stranded DNA. The widespread use of other intercalating dyes in cell and molecular biology allows for a variety of potential donor/acceptor pairs to be chosen for a particular biological application.

On the basis of these studies and our experience so far, it is not apparent that FRET offers increased sensitivity over existing methods for detecting nucleic acid hybridization (9). However, FRET has a feature not shared by any other method. In all existing methods for detecting nucleic acid hybridization, the hybrids can only be detected after removal of nonhybridized nucleic acid. FRET is different, and powerfully so, in this respect. Resonance energy transfer creates a distinctive signal in the presence of nonhybridized nucleic acid strands. The implications of this for analytical and diagnostic methods and for detecting hybridization events *in vivo* are obvious.

Finally, the approach we have described here in solution studies should be applicable to living cells by microinjecting fluorophore-tagged pairs of nucleic acids for an endogenous, complementary, nucleic acid sequence of interest (Fig. 1*b*). For example, it may prove possible to observe the progression of viral infection and replication in living cells by microinjection of appropriate fluorophore-tagged nucleic acids and observation by fluorescence microscopy and subsequent computer-enhanced video imaging techniques. Indeed, FRET microscopy has been used to monitor the association of membrane-bound probes in living cells (12) and it should be possible to use this technique for *in situ* hybridization as well.

We thank Dr. Thoru Pederson (Worcester Foundation for Experimental Biology) and Dr. Elliot Elson (Washington University, Saint Louis) for critical review of this manuscript and Christine A. McKinnon for excellent technical assistance in preparation of the figures. This research was supported by National Institutes of Health Institutional Training Grant HD07312 (to R.A.C.), National Research Service Award HD07017 (to R.A.C.), Cancer Center Core Grant P30-12708 (to the Worcester Foundation for Experimental Biology), and Grants HD23294 (to D.E.W.) and GM31562 (to P.C.Z.). Additional funding was provided by a grant from the G. Harold and Leila Y. Mathers Foundation (to P.C.Z.).

1. Forster, T. (1949) *Z. Naturforsch. A* **4**, 321–327.
2. Forster, T. (1959) *Discuss. Faraday Soc.* **27**, 7–17.
3. Stryer, L. & Haugland, R. P. (1967) *Proc. Natl. Acad. Sci. USA* **58**, 719–726.
4. Agrawal, S., Christodoulou, C. & Gait, M. J. (1986) *Nucleic Acids Res.* **14**, 6227–6245.
5. Emson, P. C., Arai, H., Agrawal, S., Christodoulou, C. & Gait, M. J. (1988) *Methods Enzymol.* **168**, in press.
6. Zamecnik, P. C., Stephenson, M. L. & Scott, J. F. (1960) *Proc. Natl. Acad. Sci. USA* **46**, 811–822.
7. Booker, T. R., Augerer, L. M., Yeu, P. H., Hershey, N. D. & Davidson, N. (1978) *Nucleic Acids Res.* **5**, 363–384.
8. Kapuscinski, J. & Darzynkiewicz, Z. (1987) *J. Biomol. Struct. Dyn.* **5**, 127–143.
9. Matthews, J. A. & Kricka, L. J. (1988) *Anal. Biochem.* **169**, 1–25.
10. Heller, M. J. & Morrison, L. E. (1985) in *Rapid Detection and Identification of Infectious Agents*, eds. Kingsbury, D. T. & Falkow, S. (Academic, New York), pp. 245–256.
11. Holowka, D. & Baird, B. (1983) *Biochemistry* **22**, 3466–3474.
12. Uster, P. S. & Pagano, R. E. (1986) *J. Cell Biol.* **103**, 1221–1234.